

# Tunneling time and weak measurement in strong field ionisation

T. Zimmermann and S. Mishra and B. Doran and D. Gordon and

A. Landsman

Research Report No. 2015-39  
November 2015

Seminar für Angewandte Mathematik  
Eidgenössische Technische Hochschule  
CH-8092 Zürich  
Switzerland

# Tunneling time and weak measurement in strong field ionisation

Tomáš Zimmermann,<sup>1,2</sup> Siddhartha Mishra,<sup>1</sup> Brent R. Doran,<sup>3</sup> Daniel F. Gordon,<sup>4</sup> and Alexandra S. Landsman<sup>1,2,5</sup>

<sup>1</sup>*Seminar for Applied Mathematics, ETH Zurich, CH-8093 Zurich, Switzerland*

<sup>2</sup>*Physics Department, ETH Zurich, CH-8093 Zurich, Switzerland*

<sup>3</sup>*Department of Mathematics, ETH Zurich, CH-8093 Zurich, Switzerland*

<sup>4</sup>*Radiation and Acceleration Physics Section, Naval Research Laboratory, Washington DC*

<sup>5</sup>*Max Planck Institute for the Physics of Complex Systems, D-01187 Dresden, Germany*

(Dated: October 21, 2015)

Tunnelling delays is a hotly debated topic, with many conflicting definitions and little consensus on when and if such definitions accurately describe the physical observables. Here we relate these different definitions to distinct experimental observables in strong field ionization, finding that two definitions, Larmor time and Bohmian time, are compatible with the attoclock observable and the resonance lifetime of a bound state, respectively. Both of these definitions are closely connected to the theory of weak measurement, with Larmor time being the weak measurement value of tunneling time and Bohmian trajectory corresponding to average particle trajectory, which has been recently reconstructed using weak measurement in a two-slit experiment[1]. We demonstrate a big discrepancy in strong field ionization between the Bohmian and the weak measurement values of tunneling time, and suggest this arises because the tunneling time is calculated for a small probability post-selected ensemble of electrons. Our results have important implications for interpretation of experiments in attosecond science, suggesting that tunneling is unlikely to be an instantaneous process.

*How much time does it take for a particle to quantum tunnel through a potential barrier?* This question has been a subject of intense theoretical debate for the last 80 years [2–7]. Time is not a quantum operator, hence, in contrast to tunneling probabilities, the tunneling time itself is, famously, not a well-defined concept in quantum mechanics. Many different definitions have been proposed, and though defined and often invoked independently of physical regime, they may actually be practically relevant only in different regimes; theoretical developments to date shed little light on which is applicable when.

Experiments measuring tunnelling of photons have found super-luminal (although non-instantaneous) barrier propagation time [8, 9], which has been explained using ideas from weak measurement [10]. In strong field ionization, the best known proposal for experimentally measuring tunneling time is the attoclock [6]. Attoclock measurements recently found sub-luminal tunneling time in helium over a wide intensity range, using two independent experimental apparatus [11]. Here we bring weak measurement to bear for the first time in strong field ionization, with an eye towards these experiments.

Recently, weak measurement was used to reconstruct the average photon trajectory in a two-slit experiment, showing that these trajectories are Bohmian [1] (a detailed theoretical discussion of the relationship between Bohmian mechanics and weak values can be found in [12]). Bohmian predictions have been found to agree in virtually every respect with the predictions of conventional quantum mechanics, tunneling time is one notable example where conventional quantum mechanics offers a number of conflicting definitions, while Bohmian me-

chanics privileges one: namely the time that the Bohmian trajectory spends between the entrance and the exit points of the potential barrier. Here, we implement some of the best-known tunneling time definitions derived within conventional quantum mechanics, and also compute the time that the Bohmian trajectory spends inside the barrier during strong field ionization. We find that Bohmian time is likely too large to correspond to tunneling time but rather agrees closely with the resonance lifetime of a bound state.

Our setting of strong field ionization of atoms is especially relevant to attosecond science experiments where tunnel ionisation is regularly used to probe electron dynamics inside atoms and molecules on the attosecond time scale [13, 14]. Interpretation of such experiments both heavily relies on the well-known tunnelling model, and, importantly, neglects the time delays associated with the tunnelling process itself. Such delays are often assumed to be instantaneous or imaginary [15], since momentum is imaginary in the classically forbidden region, which in turn leads to imaginary time [16]. This argument however, is applicable to tunneling in general [2]; and hence the need to explain how instantaneous (and therefore super-luminal) tunneling would not violate physical causality still remains. Here, we find, however, that none of the well-known approaches to tunneling delays predict instantaneous tunneling, if a full solution, rather than a saddle point approximation (such as was done in [16]), is used.

Prior work on tunneling time in strong field ionization [11] calculated four well-known tunneling time definitions (but not Bohmian time) for strong field ionization of helium by using a short range potential approximation,

which neglects the long tail of the Coulomb potential, resulting in a triangular barrier of width  $I_p/F$ , where  $I_p$  and  $F$  are the ionization potential and field strength, respectively. The problem was then solved in analogy to free propagation by matching a free wave outgoing solution to an experimental observable.

Arguably, for the purposes of calculating tunneling time, the bound state problem is fundamentally different from free propagation and therefore it is desirable to fully take account of the bound state wavefunction. Here, we fully take account of the Stark-shifted ground state wave function of the atom and fully include the Coulomb field. Our solution is exact, in the optical tunnelling limit of  $\gamma \rightarrow 0$ , for hydrogen and for helium, within the validity of a single active electron approximation. (Here,  $\gamma = \omega(2I_p)^{1/2}/F$  is the Keldysh parameter, with  $\omega$  being the frequency of the laser). We find that for the four tunnelling time definitions (but not Bohmian time), the agreement between the exact solution and the short range potential approximation, such as was implemented in [11], is very good, as long as the barrier width of the triangular barrier is similar to the exact barrier width.

These four tunnelling times are based on very different models, but can all be expressed in terms of the transmission amplitude  $T = |T|e^{i\theta}$  [5], where  $T = \psi(q_1)/\psi(q_2)$ , and  $\psi$  is the wave function value at the outer ( $q_1$ ) or inner ( $q_2$ ) classical turning point. Deriving  $T$  with respect to the the height of the potential  $V$ , and the incident energy of the particle  $E$ , one obtains: Larmor (LM) time,  $\tau_{LM}$ , the Büttiker-Landauer (BL) time,  $\tau_{BL}$ , the Eisenbud-Wigner (EW) time,  $\tau_{EW}$ , and the Pollack-Miller (PM) time,  $\tau_{PM}$  (for detailed discussion, see for example [4, 7]). The first two times depend on the potential and have been called the *resident (or dwell) time*,

$$\tau_{BL} = -\hbar \partial \ln |T| / \partial V; \quad \tau_{LM} = -\hbar \partial \theta / \partial V. \quad (1)$$

The other two times depend on the incident energy of the particle and have been called the *passage time*,

$$\tau_{PM} = \hbar \partial \ln |T| / \partial E; \quad \tau_{EW} = \hbar \partial \theta / \partial E. \quad (2)$$

The Buttiker-Landauer time [3] and the Pollack-Miller time [?] depend on the probability of transmission, and can therefore be well approximated using WKB. The Buttiker-Landauer time is actually closely related to the Keldysh time (see [7] for explanation), while the Pollack-Miller time corresponds to the imaginary part of the time average of the flux-flux correlation function. The other two times, namely the Larmor [?] and the Eisenbud-Wigner times [?], are phase-dependent. This phase-dependence makes the evaluation considerably more difficult, as the usual saddle-point and WKB approaches fail (see [7] for a discussion) and a complete solution of the transmission amplitude is necessary. The Larmor time was originally defined as given by the precession of the electron spin inside a rectangular magnetized barrier

[?], but has since been generalized to arbitrary barriers [?]. The Eisenbud-Wigner time is well-known in single photon ionization (for a detailed treatment, see for example an excellent recent review by Pazourek, Nagele, and Burgdoerfer [?])

In addition to the four definitions above, we also compute the Bohmian tunneling time, defined as the time which it takes a Bohmian trajectory to pass the region between the two classical turning points. In the Bohmian formalism, the wavefunction is expressed as  $\psi(\vec{r}, t) = R(\vec{r}, t)e^{iS(\vec{r}, t)/\hbar}$ , where  $R$  and  $S$  are real valued. The Bohmian trajectory is determined by the probability density, given by  $\rho(\vec{r}, t) = R(\vec{r}, t)^2$  and velocity, given by  $\vec{v} = \nabla S/m = \vec{j}(\vec{r}, t)/\rho(\vec{r}, t)$  [17, 18], where  $\vec{j} = (i/2)(\psi \nabla \psi^* - \psi^* \nabla \psi)$  is the probability flux. Since flux is constant for solutions of the stationary Schrödinger equation, the Bohmian time is computed as

$$\tau_{\text{Bohmian}} = \frac{1}{j} \int_{q_1}^{q_2} \rho dq. \quad (3)$$

The Bohmian time, as well as the other times, is computed in the adiabatic limit, by solving the Schrödinger equation for the hydrogen atom in the homogeneous electric field  $F$ :

$$\left( -\frac{\Delta}{2} + \frac{1}{r} - Fz \right) \psi = E\psi \quad (4)$$

The above equation is separable in the parabolic coordinates  $\xi = r+z$ ,  $\eta = r-z$ , and  $\phi = \arctan(y/x)$  [19]. Substituting  $\psi(\xi, \eta, \phi) = (\xi\eta)^{-1/2} \chi_1(\xi) \chi_2(\eta) e^{-im\phi}$  into Eq. (4), we obtain two one-dimensional equations for  $\chi_1(\xi)$  and  $\chi_2(\eta)$

$$-\frac{1}{2} \frac{\partial^2 \chi_1}{\partial \xi^2} + \left( \frac{m^2 - 1}{8\xi^2} - \frac{\beta_1}{2\xi} + \frac{F\xi}{8} \right) \chi_1 = \frac{E}{4} \chi_1, \quad (5)$$

$$-\frac{1}{2} \frac{\partial^2 \chi_2}{\partial \eta^2} + \left( \frac{m^2 - 1}{8\eta^2} - \frac{\beta_2}{2\eta} - \frac{F\eta}{8} \right) \chi_2 = \frac{E}{4} \chi_2, \quad (6)$$

which are coupled by the separation constants  $\beta_1$  and  $\beta_2$  satisfying  $\beta_1 + \beta_2 = 1$ . Whereas all solutions of Eq. (5) are bound and the energy spectrum is discrete, Eq. (6) has unbound solutions with a continuous energy spectrum. The ionization is therefore described by Eq. (6) and the coordinate  $\eta$  naturally corresponds to the tunneling degree of freedom. In order to describe the steady-state ionization process, one first has to find the solution of Eq. (6) which is outgoing for  $\eta \rightarrow \infty$ . Details of the procedure used to find the outgoing solution of Eq. (6) may be found in the Supplemental information.

In addition to the exact solution of the Schrödinger equation (4), tunneling times were computed using the short-range potential approximation, as was previously done in [11]. The short-range potential is a consequence of the Strong Field Approximation (SFA), originally introduced by Keldysh [20], and in the adiabatic

limit reduces to the propagation through a static one-dimensional triangular barrier [? ], given by Eq. (7) below.

Even though the SFA may be solved analytically, in this work we treat the SFA numerically, in the same way for helium and hydrogen, by solving the Schrödinger equation for the triangular barrier

$$-\frac{1}{2} \frac{\partial^2 \chi_s}{\partial \eta^2} + V_{\text{SFA}}(\eta) \chi_s = E \chi_s, \quad (7)$$

where  $V_{\text{SFA}}(\eta) = -F\eta$  for  $\eta > 0$  is the part of the potential corresponding to the triangular barrier and  $V_{\text{SFA}}(\eta) = 2E$  for  $\eta < 0$  corresponds to the potential well holding the initial “bound” state. (Note that as long as the classical turning point is produced at  $\eta = 0$ , the exact value of  $V_{\text{SFA}}(\eta)$  for  $\eta < 0$  is irrelevant for all the tunneling times.) The energy  $E$  is equal to the exact resonance energy in case of hydrogen. (In case of helium, it is calculated according to Eq. (S8) in Supplemental.) The equation is solved in a way analogous to Eq. (6), using an outgoing Airy function (which, in this case, is an exact solution) to start the integration.

Tunneling times of hydrogen are shown in Fig. 1. Note that all these times are significantly slower than superluminal, which is less than 10 attoseconds (since the barrier width, given approximately by  $I_p/F$ , is less than 50 au). Bohmian tunneling time is, especially for weaker  $F$ , several orders of magnitude higher than the other tunneling times. This points to the important difference between the time based on Bohmian trajectories and the other definitions of the tunneling times. The Bohmian trajectories—following the probability density—reflect the time needed by the entire wave function to escape through the barrier whereas the other times reflect the time needed by each small fraction to pass the barrier. The Bohmian times were therefore found to be related to lifetimes of corresponding resonances: indeed the agreement between the Bohmian times and lifetimes is nearly perfect. (The resonance lifetimes  $\tau_L$  were computed from the resonance widths  $\Gamma$  taken from Ref. 21 using  $\tau_L = 1/\Gamma$ . Note that for stronger  $F$  the agreement must necessarily deteriorate, since  $\Gamma$  stays finite even when the barrier length and Bohmian tunneling time approaches zero.) Interestingly, the SFA performs substantially worse for Bohmian trajectories than it does for other tunneling times, pointing to much stronger sensitivity of the Bohmian time on the exact shape of the barrier.

As can be seen from Fig. 1, the agreement between the short-range potential approximation (labeled as SFA in the figure) and the exact solution breaks down as the field strength increases. This can be understood by considering the actual barrier width compared to the width of the triangular potential,  $I_p/F$ , which comes out of SFA. In particular, as one approaches the over-the-barrier-ionization (OBI) regime, the actual barrier disappears,

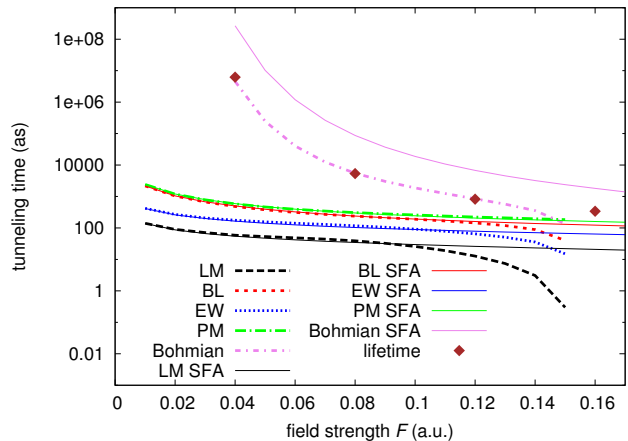


FIG. 1. Tunneling times of hydrogen using the exact parabolic solution, SFA, and exact resonance energies. The resonance lifetimes were taken from Ref. 21.

while the approximation always predicts a triangular barrier of width  $I_p/F$ . This also explains why Fig. 2 shows very good agreement between SFA and the exact solution in helium. In particular, helium stays well within OBI regime for the range of field strengths shown in Fig. 2; and hence the actual barrier shape is close to  $I_p/F$ . In general, we found the four tunneling time definitions to be much less sensitive on the exact barrier shape than ionization probabilities.

A recent work dealing exclusively with the attoclock approach to measuring tunneling time – rather than with the more general theoretical definitions computed here – suggests tunneling in hydrogen is instantaneous [16]. However, although Torlina et al [16] deal extensively with ionization time (corresponding with the time the electron appears at the tunnel exit), no explicit definition of tunneling time is provided or discussed in the paper. Given that the authors in [16] also question the key “time zero” assumption normally used in the attoclock extraction of tunneling time, without providing an alternative “time zero”, it seems the information presented in [16] is insufficient to definitively conclude instantaneous tunneling (see Supplemental IV for a more detailed discussion).

For helium, the time-independent Schrödinger equation is not separable in the parabolic coordinates. Nevertheless, it may be separated approximately using the TIPIS model [22] (See Supplemental for details on computation). The tunneling times of helium plotted in Fig. 2 are, especially for weak fields, relatively similar to those of hydrogen. Mostly due to higher lying tunneling ionization threshold, the agreement between TIPIS and the SFA is better in helium than in hydrogen. Also, the TIPIS tunneling times go to zero at much higher values of  $F$  than for hydrogen – outside of the range studied here. Bohmian times (not shown) are, similarly to hydrogen, several orders of magnitude higher than the other tun-

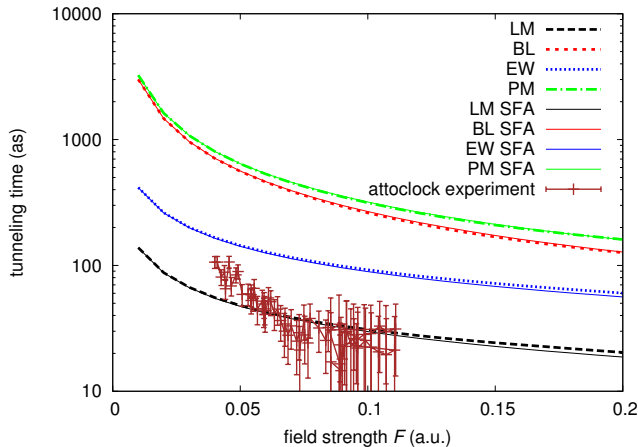


FIG. 2. Tunneling times of helium using TIPIS and the SFA with resonance energies computed using the second-order perturbation theory in comparison with the attoclock experiment.

neling times.

Our numerical results are compared with the recent attoclock experimental data in Fig. 2. The attoclock uses elliptically polarized light to obtain an electron momenta distribution in the plane of polarization, following ionization of gas [11, 23–26]. Tunneling time is experimentally defined as corresponding to the angle of rotation in the electron momenta distribution, relative to what would be expected if the most probable electron trajectory appears at the tunnel exit at the peak of the laser field (for a detailed description of the attoclock concept, see for example [27]). The exact location of the attoclock data points in Fig. 2 may vary up to 100 attoseconds, depending on the calibration method and intensity, hence not excluding super-luminal values [16]. Nevertheless, it is clear that, among the approaches to tunneling time discussed here, only Larmor time can be compatible with the attoclock measurements, since the other times lie significantly outside the experimental range.

It is important to note that the attoclock set-up is only able to reliably extract tunneling times that are significantly shorter than the laser period. Hence, for the wavelength of 735 nm (corresponding to the experimental data plotted in Fig. 2), the attoclock set-up would not have been able to reliably access tunneling times significantly longer than 100 attoseconds (see [?] for additional explanation). In this case, much longer mid-IR pulses may be a good alternative, particularly since they correspond to a smaller  $\gamma$  regime. An interesting alternative model that bypasses this limitation by using a stationary barrier and an XUV pulse to clock the start of the tunneling process (with the IR pulse subsequently used for streaking) was recently proposed in [?].

Both the calibration and the interpretation of the attoclock measurements has recently become a topic of much

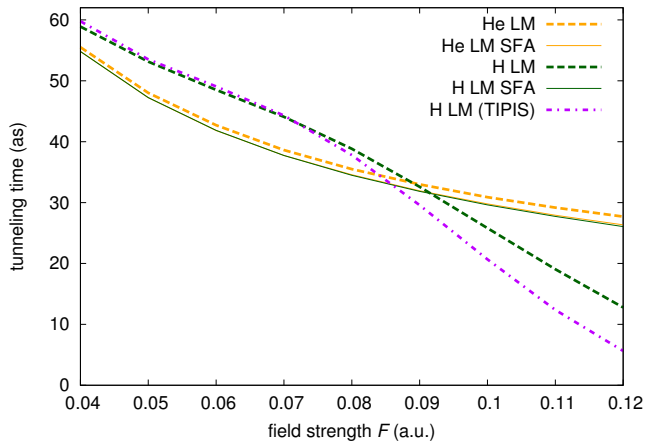


FIG. 3. LM times of hydrogen and helium.

discussion, with most recent work [16] proposing an alternative method to the previously used TIPIS model [22]. Their method relies on the non-adiabatic model called ARM [28], which gives similar results (i.e. similar initial conditions at the tunnel exit [28]) to another well-known non-adiabatic model called PPT [29]. (Interestingly TIPIS and PPT, and therefore the ARM, agree within one degree in their predictions for the experimental data plotted in Figure 2 [26]. Hence, the ‘attoclock experiment’ data points plotted in Figure 2 are robust to whether an adiabatic or non-adiabatic theory is applied to the attoclock measurements when extracting tunneling delays.) Here, rather than address the possible interpretations of attoclock measurements, we implement different theoretical predictions for tunneling time itself, with the motivation that they can later be related to different experimental observables, hence clarifying the experimental context under which one theoretical definition or another is appropriate.

Figure 3 compares, in closer detail, the LM times of hydrogen and helium. Interestingly, in the SFA, the LM times of both atoms are almost identical (to the point that it is difficult to discern between them in the figure). Higher resolution of Fig. 3 clearly demonstrates that, in the intensity range studied, the SFA does a better job in case of helium than in case of hydrogen. In addition, Fig. 3 allows for assessing effects on accuracy of using the second-order energy and second-order separation constant in TIPIS by means of comparison with the exact solution in parabolic coordinates in hydrogen.

Following the Feynman path integral approach, the Larmor time can be expressed as [4]

$$\tau_{LM} = Re \frac{\langle \psi_f | \tau | \psi_i \rangle}{\langle \psi_f | \psi_i \rangle} = Re (\tau_T^\Omega) \quad (8)$$

where  $\psi_i$  and  $\psi_f$  correspond to initial and final states, respectively, and  $\tau_T^\Omega$  is the complex average tunneling time defined within the path integral approach [30]. It

is clear from the above definition that the Larmor time corresponds to the weak measurement value of tunneling time, since the weak measurement value of an observable,  $a$ , is given by:  $Re(\langle\psi_f|\hat{a}|\psi_i\rangle/\langle\psi_f|\psi_i\rangle)$  [12, 31].

The significant discrepancy between the Bohmian and the Larmor times may be understood by considering that the weak value can differ considerably from the ensemble average obtained using strong value measurements, if this ensemble average is calculated by post-selecting only those results for which a later strong measurement reveals the system to be in a state  $|\psi_f\rangle$  [12]. This is indeed the case in the attoclock strong field ionization experiment, where tunneling time is extracted from a small fraction of tunnelled electrons, all corresponding to the same post-selected state, given by  $|\psi_f\rangle = |p_0\rangle$ , where  $p_0$  corresponds to the most probable momentum observed at the detector.

On the other hand, the density of Bohmian trajectories directly represents the quantum probability density. In addition, all Bohmian trajectories representing solutions of the time-independent Schroedinger equation are the same (except for the time shift) and the time they spend in a given region of space is directly proportional to the probability density. Therefore, Bohmian time can be viewed as an ensemble average (as it is weighted by the probability density) and indeed it corresponds to the total ionization time of the state. Therefore, if the fraction of electrons which end up in such a final state  $|p_0\rangle$  is very small (corresponding to a low probability of ionization), the Bohmian time can differ considerably from the weak measurement value of tunneling time. Moreover, since the attoclock experiment intentionally avoids the saturation regime, only a small fraction of the initial bound state wave-packet makes it to the detector, explaining why it is the Larmor time, rather than the Bohmian time, which may be possible to access with the attoclock.

This research was supported by ETH Research grant no. ETH-03 09-2.

- 
- [1] S. Kocsis, B. Braverman, S. Ravets, M. J. Stevens, R. P. Mirin, L. K. Shalm, and A. M. Steinberg, *Science* **332**, 1170 (2011), URL <http://www.sciencemag.org/content/332/6034/1170.abstract>.
- [2] R. Landauer, *Nature* **567** (1989).
- [3] M. Büttiker and R. Landauer, *Physical Review Letters* **49**, 1739 (1982).
- [4] R. Landauer and T. Martin, *Reviews of Modern Physics* **66**, 217 (1994).
- [5] N. Yamada, *Physical Review Letters* **93** (2004).
- [6] P. Eckle, A. N. Pfeiffer, C. Cirelli, A. Staudte, R. Dörner, H. G. Muller, M. Büttiker, and U. Keller, *Science* **322**, 1525 (2008), URL <http://www.sciencemag.org/content/322/5907/1525.abstract>.
- [7] A. S. Landsman and U. Keller, *Physics Reports* **547**, 1 (2015), URL <http://www.sciencedirect.com/science/article/pii/S0370157314003159>.
- [8] C. Spielmann, R. Szipöcs, A. Stingl, and F. Krausz, *Physical Review Letters* **73**, 2308 (1994).
- [9] A. M. Steinberg, P. G. Kwiat, and R. Y. Chiao, *Physical Review Letters* **71**, 708 (1993).
- [10] A. M. Steinberg, *Physical Review Letters* **74**, 2405 (1995).
- [11] A. S. Landsman, M. Weger, J. Maurer, R. Boge, A. Ludwig, S. Heuser, C. Cirelli, L. Gallmann, and U. Keller, *Optica* **1**, 343 (2014), URL <http://www.opticsinfobase.org/optica/abstract.cfm?URI=optica-1-5-343>.
- [12] H. M. Wiseman, *New Journal of Physics* **9** (2007).
- [13] E. Goulielmakis, Z.-H. Loh, A. Wirth, R. Santra, N. Rohringer, V. S. Yakovlev, S. Zherebtsov, T. Pfeifer, A. M. Azzeer, M. F. Kling, et al., *Nature* **466**, 739 (2010), URL <http://dx.doi.org/10.1038/nature09212>.
- [14] A. Wirth, M. T. Hassan, I. Grguraš, J. Gagnon, A. Moulet, T. T. Luu, S. Pabst, R. Santra, Z. A. Alahmed, A. M. Azzeer, et al., *Science* **334**, 195 (2011), URL <http://www.sciencemag.org/content/334/6053/195.abstract>.
- [15] M. Lein, *Nature* **485**, 313 (2012), URL <http://dx.doi.org/10.1038/485313a>.
- [16] L. Torlina, F. Morales, J. Kaushal, I. Ivanov, A. Kheifets, A. Zielinski, A. Scrinzi, H. G. Muller, S. Sukiasyan, M. Ivanov, et al., *Nat Phys* **11**, 503 (2015), URL <http://dx.doi.org/10.1038/nphys3340>.
- [17] D. Bohm, *Physical Review* **85** (1952).
- [18] C. L. Lopreore and R. E. Wyatt, *Physical Review Letters* **82**, 5190 (1999).
- [19] L. D. Landau and E. M. Lifshitz, *Quantum Mechanics: Nonrelativistic theory* (Pergamon Press, 1991).
- [20] L. Keldysh, *JETP* **20**, 1307 (1965).
- [21] R. J. Damburg and V. V. Kolosov, *J. Phys. B* **9**, 3149 (1976).
- [22] A. N. Pfeiffer, C. Cirelli, M. Smolarski, D. Dimitrovski, M. Abu-samha, L. B. Madsen, and U. Keller, *Nat. Phys.* **8**, 76 (2012).
- [23] A. S. Landsman, C. Hofmann, A. N. Pfeiffer, C. Cirelli, and U. Keller, *Physical Review Letters* **111** (2013).
- [24] C. Hofmann, A. S. Landsman, C. Cirelli, A. N. Pfeiffer, and U. Keller, *Journal of Physics B: Atomic, Molecular and Optical Physics* **46**, 125601 (2013).
- [25] R. Boge, C. Cirelli, A. S. Landsman, S. Heuser, A. Ludwig, J. Maurer, M. Weger, L. Gallmann, and U. Keller, *Physical Review Letters* **111** (2013).
- [26] A. S. Landsman and U. Keller, *Journal of Physics B: Atomic, Molecular and Optical Physics* **47**, 204024 (2014).
- [27] L. Gallmann, C. Cirelli, and U. Keller, *Annual Review of Physical Chemistry* **63**, 447 (2012), URL <http://dx.doi.org/10.1146/annurev-physchem-032511-143702>.
- [28] J. Kaushal and O. Smirnova, *Physical Review A* **88** (2013).
- [29] A. Perelomov, V. Popov, and M. Terent'ev, *JETP* **23** (1966).
- [30] D. Sokolovski and L. M. Baskin, *Physical Review A* **36**, 4604 (1987).
- [31] Y. Aharonov, D. Z. Albert, and L. Vaidman, *Physical Review Letters* **60**, 1351 (1988).

## Recent Research Reports

Nr.	Authors/Title
2015-29	G. S. Alberti and S. Dahlke and F. De Mari and E. De Vito and S. Vigogna Continuous and discrete frames generated by the evolution flow of the Schrödinger equation
2015-30	P. Grohs and G. Kutyniok and J. Ma and P. Petersen Anisotropic Multiscale Systems on Bounded Domains
2015-31	R. Hiptmair and L. Scarabosio and C. Schillings and Ch. Schwab Large deformation shape uncertainty quantification in acoustic scattering
2015-32	H. Ammari and P. Millien and M. Ruiz and H. Zhang Mathematical analysis of plasmonic nanoparticles: the scalar case
2015-33	H. Ammari and J. Garnier and L. Giovangigli and W. Jing and J.K. Seo Spectroscopic imaging of a dilute cell suspension
2015-34	H. Ammari and M. Ruiz and S. Yu and H. Zhang Mathematical analysis of plasmonic resonances for nanoparticles: the full Maxwell equations
2015-35	H. Ammari and J.K. Seo and T. Zhang Mathematical framework for multi-frequency identification of thin insulating and small conductive inhomogeneities
2015-36	H. Ammari and Y.T. Chow and J. Zou Phased and phaseless domain reconstruction in inverse scattering problem via scattering coefficients
2015-37	A. Kunoith and Ch. Schwab Sparse adaptive tensor Galerkin approximations of stochastic PDE-constrained control problems